2024 IEEE International Conference on Robotics and Automation (ICRA 2024)
May 13-17, 2024. Yokohama, Japan

Lightweight and Compliant Bilateral Teleoperation System with Anthropomorphic Arms for Aerial and Ground Service Operations

Alejandro Suarez[1], Antonio Gonzalez-Morgado[1], and Anibal Ollero[1], *IEEE Fellow*

***Abstract*— This paper presents a bilateral teleoperation system based on smart servos for the realization of dexterous manipulation tasks with aerial robots or in ground service applications, facilitating the transferability of cognitive capabilities of human workers to robots operating remotely or in high altitude workspaces. The system consists of a pair of lightweight and compliant anthropomorphic dual arm manipulators (LiCAS) in leader-follower configuration. The leader dual arm (LDA) captures the movements of the operator's arms to obtain the desired joint references, sent to the follower dual arm (FDA) to reproduce in a natural and intuitive way the manipulation task. A model of the smart servos is derived, exploiting the feedback from the FDA actuators to provide the kinesthetic feedback to the LDA, using the pulse width modulation signal (PWM) along with the joint speed to estimate the interaction torque. The mechanical joint compliance of the FDA allows the passive accommodation of the arms to the physical interactions with the manipulated objects or the environment, whereas the very low weight of the arms (1.0 kg LDA, 2.5 kg FDA) and the human-size and human-like kinematics facilitate their use in a wide variety of applications. The performance of the system is evaluated using an industrial task board for benchmarking, and in two illustrative bimanual aerial manipulation tasks.**

I. INTRODUCTION

Teleoperation of robot manipulators is a convenient solution adopted when the complexity of the task carried out in remote workspaces does not allow its automation in a feasible or reliable way, but it is necessary to incorporate the cognitive capabilities and skills of human workers. It is also typical in industrial inspection and maintenance that human operators prefer to have a certain level of control over the robot for accessing points of interest of the infrastructures, so, based on their knowledge, experience and perception of the environment, the actions of the robot are conveniently selected. Space robotics is one of the most representative domains where methods and techniques for robot teleoperation have been extensively studied [1], [2], [3], adopting later some concepts to the aerial manipulation field [4], [5], where time delays are much lower. The development of novel teleoperation interfaces for robotic manipulators, particularly humanoids [6], is of further interest as a way to transfer human manipulation skills to robots capable of learning from demonstration [7]. However, teleoperation interfaces relying on industrial robotic arms may be unpractical in many cases due to the high cost, weight and difficulty for transportation and handling compared to very low weight robotic arms built with smart servo actuators developed for the realization of dexterous aerial manipulation tasks [8], [9], [10].

Authors are with GRVC Robotics Laboratory, School of Engineers, University of Seville, 41092 Seville, Spain asuarezfm@us.es, mantonio@us.es, aollero@us.es

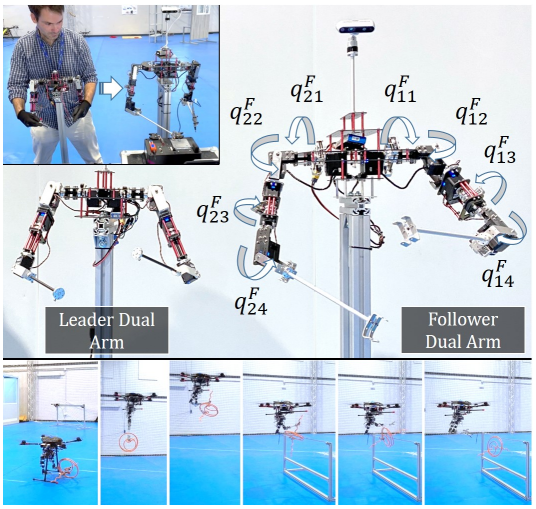

Fig. 1. Lightweight and compliant anthropomorphic dual arm teleoperation system in leader/follower configuration (1.0 / 2.5 kg weight). Benchmark evaluation with industrial task board (up-left). Application to installation of flexible device on a power line section using both arms on flight (down).

Depending on the intended task, type of feedback, and other ergonomic factors, it is possible to find a wide variety of teleoperation devices, including joysticks [11][12], haptic devices [13][14], wearable devices [15][16], exoskeletons [17][18], or robotic arms [19][20]. In this case, the direct replication of movements enables a comfortable and intuitive manipulation, removing the need for special training and facilitating the learning-by-imitation methods [21][22]. Some of the latest developments in bilateral teleoperation systems focus on giving the user a haptic feedback by incorporating force sensors in the follower device. In [13], a dual-arm teleoperation architecture with haptic and visual feedback is introduced to enhance the operator immersion in surface treatment tasks, whereas in [14] a similar approach is applied to suturing in minimally invasive surgery. An important part of such teleoperation schemes is the study of the stability of the communication channel, which is usually addressed through the passivity property [12][23].

The main contribution of this paper is the development and experimental validation of a bilateral teleoperation system for the realization of dexterous bimanual manipulation tasks, either on flight [8], [9], in ground [20], or in cable suspended configurations [24], [25], using a pair of lightweight and compliant anthropomorphic arms (LiCAS) in leader-follower configuration, as shown in Figure 1. The proposed scheme facilitates the replication of dexterous manipulation task con-

ducted by the human workers, providing kinesthetic feedback by estimating the torque from the measurements given by the smart servo actuators without introducing additional sensors. This implementation reduces significantly the cost, weight and complexity of the system compared to solutions based on industrial robotic manipulators. The system is validated in several tests, including benchmarking with an industrial task board [26], the installation of a deformable object with complex geometry of a power line, and grasping-dropping a parcel on flight for logistics applications.

The rest of the paper is organized as follows. Section II motivates the design of the system proposed here. Section III describes the mechatronic system and its modeling, presenting in Section IV the teleoperation scheme. Experimental results are reported in Section V, summarizing the conclusions and future work in Section VI.

II. MOTIVATION

The dual arm teleoperation system presented in this work, depicted in Figure 1, is developed in the context of two European projects, combining two scientific topics closely related. On the one hand, cognition in aerial robotic manipulation [27] is explored as part of the AERIAL-CORE[1] project [28], considering the application of aerial manipulation robots equipped with dexterous robotic arms for the realization of maintenance operations on power lines, replacing human workers in highly risky tasks such as the installation of bird flight diverters [10], a relevant activity with strong environmental and economic impact due to the vast extension of this critical infrastructure and the regulation imposed for protecting bird species against collision and electrocution. On the other hand, transferability, understood as the ability of robots to share skills or knowledge among them, plays a key role as part of the European Robotics and Artificial Intelligence Network (euROBIN[2]), involving different types of robots, including aerial robots, industrial manipulators, and other ground mobile manipulators.

The need for an anthropomorphic teleoperation interface [6] as the one presented here is therefore motivated by the necessity to transfer the cognitive skills of human workers [29] to aerial manipulation robots [30] intended to conduct complex dexterous tasks [25] that, in practice, cannot be easily automated, incorporating haptic feedback [31], [32], [33] to extend the situational awareness and allow the robot to learn behaviours from the operator, for example how to react in case of collision or overload.

More particularly, the solution proposed in this paper considers the following key contributions:

- Facilitating the transportation by making the teleoperation interface very lightweight and even wearable for human operators doing field work.
- Reducing the cost by using smart servo actuators like Herkulex [8], [30], [10] or Dynamixel [34], [35], whose price is one order of magnitude lower compared to industrial-grade actuators built with Harmonic Drives.
- Allow the natural replication of the human motions while resulting intuitive and comfortable for the users, avoiding intensive training or fatigue during its use.

One of the positive aspects derived from the significant challenges faced in aerial robotic manipulation associated to the limited payload capacity, dynamic coupling, physical interactions on flight, and other issues associated to the use of multi-rotors, is that some of the resulting methods and technologies may be of interest for ground service robotics, where conventional methods do not have to overcome these inconveniences. Therefore, in order to extend its possible application to ground domains, the performance of the teleoperation system will be validated using an industrial taskboard developed for benchmarking purposes [26].

III. LEADER-FOLLOWER DUAL ARM SYSTEM

A. System Description

The leader-follower manipulation system shown in Figure 1 consists of a couple of lightweight and compliant anthropomorphic arms (LiCAS[3]) built with smart servo actuators, following the design principles derived from our previous works [8], [9]. Both arms implement the anthropomorphic kinematics described in [8], with two main links (upper arm and forearm), human size, and four joints for end effector positioning: 1) shoulder flexion/extension, 2) shoulder adduction/abduction, 3) medial/lateral rotation, and 4) elbow flexion/extension. The kinematics of both arms is depicted in Figure 2. Here q_{ij} denotes the rotation angle of the j-th joint of the i-th arm, where $i = \{1,2\}$ is the arm index (left/right), and $j = \{1,2,3,4\}$ is the joint index, using superscript $\{L,F\}$ for denoting the leader and follower arms, respectively. The angular speed of the joint servos is denoted by ω_{ij}, whereas $pwm_{ij} \in [-1,1]$ represents the normalized duty cycle of the pulse width modulation signal (PWM) also provided by the servo actuator, which can be used as estimation of the torque exerted by the motor (see next subsection).

The Leader Dual Arm (LDA), handled by the human operator (HOP), is built with the Herkulex DRS-0201 servos due to their lower cost and low gearbox friction, so it is comfortable for the user to operate when the torque control of the actuator is disabled, whereas the Follower Dual Arm (FDA) employs the Herkulex DRS-0402/0602 servos to provide higher payload capacity (0.7 kg) and accurate velocity measurements as these models integrate velocity encoders on the motor side. The FDA integrates a compact spring-lever transmission for providing mechanical joint compliance with relatively low stiffness ($[15,10,5,10]$ Nm/rad), allowing joint deflections up to 15 degrees. Passive compliance is exploited here to allow the accommodation of the arms to possible overloads raised during the realization of bimanual manipulation tasks involving contact forces with the environment, or in closed kinematic chains (see [8], [24] for more details), at expenses of reducing the positioning accuracy of the end effector to $5-20$ mm depending on the grasped load.

[1] AERIAL-CORE project webpage: https://aerial-core.eu/

[2] euROBIN project webpage: https://www.eurobin-project.eu/

[3] LiCAS Robotic Arms webpage: https://licas-robotic-arms.com/

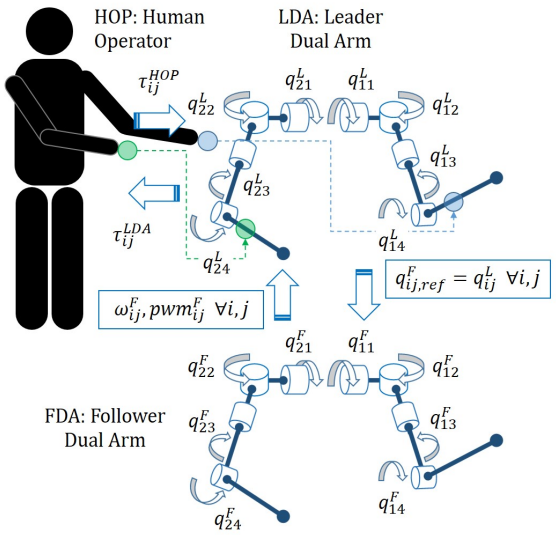

Fig. 2. Model of bilateral kinesthetic teleopreation scheme with anthropomorphic arms. The human operator (HOP) grabs the leader dual arm (LDA) at the forearm to transmit the desired motion, sent as angular position reference joint by joint to the servos of the follower dual arm (FDA), providing as haptic feedback the joint speed and PWM used for estimating the exerted effort, transmitted to the HOP through the LDA servos.

B. Servo Model

The proposed teleoperation scheme is designed taking into account the control capability and feedback availability of the smart servo actuators employed in the LDA and FDA. Note tha the concept of smart servo is taken from Dynamixel and Herkulex, the two main brands that develop this kind of actuators. These servos take as input two parameters: the goal position/speed $\theta_{ij,ref}$, and play time PT, that is, the time required to reach the goal position. Note that the Herkulex DRS-0402/0602 can be controlled in both position or velocity modes. Each time a servo receives a data packet with these parameters, the controller embedded in the actuator generates a trapezoidal velocity profile that satisfies both constraints. In order to achieve smooth motions, the velocity over-ride (VOR) mode of the servos (see users' manual) is enabled, updating the position references at the mid point of the velocity profile to avoid discontinuities. The actuator provides as feedback its current position θ_{ij}, speed $\omega_{ij} = \dot{\theta}_{ij}$, and the duty cycle of the PWM (pulse width modulation) signal generated by the controller. Note that the PWM is a normalized value that allows to compare the relative torque of different servo models. Figure 3 represents the model of the compliant servo implemented in the FDA joints. This is not integrated in the LDA since the interactions with the human are already compliant.

Since the PWM signal represents the mean current (or percentage with respect to the stall current) injected to the DC motor i, and this is proportional to the motor torque τ_m, it is possible to estimate the servo torque τ_s at the output shaft (subscripts and superscripts are omitted for clarity):

$$\tau_s = N\tau_m - \tau_f \ ; \ \tau_m = k_{mp} pwm \quad ; \quad pwm \in [-1,1] \qquad (1)$$

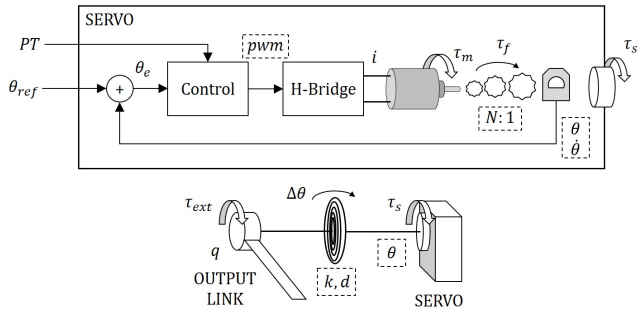

Fig. 3. Block diagram representing the compliant servo joint. Measurable signals or known parameters are marked with dashed line.

where N is the reduction ratio, τ_f is the gearbox friction, and k_{pm} is the PWM-torque constant. The friction torque can be expressed as the sum of a Coulomb and damping term:

$$\tau_f = bsign(\dot{\theta}) + c\dot{\theta} \qquad (2)$$

where b and c are constants whose value can be experimentally determined by applying known loads.

The compliant transmission mechanism introduced between the servo horn and the output link, whose angular position is denoted as q, is assimilated to a series elastic actuator in such a way that the transmitted torque is related to the joint deflection angle $\Delta\theta$ as follows:

$$\tau_{ext} = \tau_s = k\Delta\theta + d\Delta\dot{\theta} \quad ; \quad \Delta\theta = \theta - q \qquad (3)$$

where k and d are the torsional stiffness and damping coefficients. The deflection [8], [24] represents the angular deviation in the output link w.r.t. the servo shaft due to the torsion of the spring, caused by any torque acting on the joint. This angle can be measured integrating encoders in the joints [24], requiring gravity compensation to improve the positioning accuracy at the end effector [36]. Note that for the LDA, $q_{ij} = \theta_{ij} \ \forall i,j$ since all the joints are stiff. The servo model is complete including the output link dynamics which comprises the inertia, gravity, and external torque:

$$\tau_{ext} = J\ddot{q} + mgl\sin(q) \qquad (4)$$

where J, m, and l are the joint inertia, mass, and length of the center of mass, respectively.

IV. TELEOPERATION SCHEME

A. General Architecture

The kinesthetic teleoperation scheme considered in this work, with two dual arm systems (leader and follower) of identical kinematic configuration, allows the direct and independent control of all the joints of the arms, in such a way that the operator commands and receives haptic feedback in the joint space, rather than in the task space. Therefore, the teleoperation scheme will be implemented at joint level, as depicted in Figure 4. Sub-indices i and j are thus omitted for more clear notation. The human operator (HOP) commands the desired velocity of the leader servo

actuator (LSA), ω^L, exerting a torque τ^H that compensates the opposition of the servo due to friction and gravity, as well as the torque received from the follower side, $\overline{\tau}^L$. The LSA controller, detailed in next subsection, converts the torque into a corresponding velocity reference for the servo, ω^L_{ref}, taken as input by the servo actuator. The velocity reference and feedback sent to / received from the follower side are transmitted through a communication channel characterized by a forward / backwards delay, assumed to be multiple of the sampling period, that is, $T_f = k_f T$ and $T_b = k_b T$, where $k_f, k_b \in \mathbb{N}_{>0}$. This delay comprises the component associated to the wireless communication link, as well as the delay associated to the serial communication of the servo actuators.

The follower servo actuator (FSA) receives the delayed velocity reference $\overline{\omega}^F$, giving as output the angular velocity $\omega^F = \dot{\theta}^F$ transmitted to the environment (ENV) through the spring-lever transmission mechanism (see Eq. (3)). Taking into account that the maximum update rate for the servos is around 70 Hz, imposed by the serial interface, and the typical wireless communication delays, below 100 ms, it can be assumed that $k_f,\ k_b \in [1, 10]$. The impact of variable delays in this range is in practice relatively low due to the smoothing effect of the VOR control mode of the smart servos.

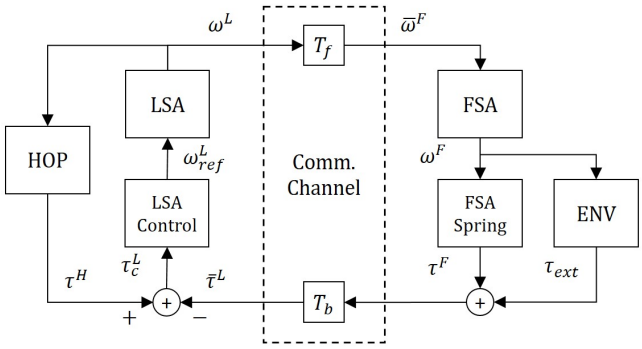

Fig. 4. Bilateral teleoperation scheme based on force-position architecture.

B. LSA Controller

The goal of the Leader Servo Actuator controller block shown in Figure 4 is to generate the appropriate velocity references for the LSA based on two factors: 1) the intention of the human operator expressed through the transmitted torque τ^H, and 2) reflect the effort of the follower actuator τ^F along with the external wrenches acting on it, τ^{ext}. The torque at the input of the LSA controller is then:

$$\tau^L_c(n) = \tau^H(n) - \tau^F(n-k_b) - \tau_{ext}(n-k_b) \tag{5}$$

The velocity reference computed by the LSA controller, ω^L_{ref}, is thus the sum of two terms, a first one that compensates the torque of the HOP and the dynamics of the own LSA, and a second term that accounts the FSA interactions:

$$\begin{aligned}\omega^L_{ref}(n) = &-k^L_\tau \tau^L(n) + k^L_\omega \omega^L(n) - \\ &- k^F_\tau \tau^F(n-k_b) + k^F_\omega \omega^F(n-k_b)\end{aligned} \tag{6}$$

where τ^L and τ^F are obtained from the PWM signal of the leader/follower servos, as in Eq. (1), whereas k_τ and k_ω are the corresponding torque/velocity gains that determine the sensitivity of the teleoperation interface. The haptic feedback for the HOP corresponds to the torque generated by the LSA, which can be controlled directly through the servo position relying on the PID controller embedded in the servo, $\tau^L_c = K_p q^L$. Here K_p is the equivalent LSA joint stiffness, whereas the integral and derivative gains are set to zero. The angular speed of the servos in Eq. (6) is included to provide a more comfortable and smooth interaction for the operator.

C. Passivity Analysis

The passivity analysis of the developed teleoperation system can be assimilated to the position-force architecture in [12] and to the work done in [23] for series elastic actuators, as is the case of the FDA. A dynamic system like the servo actuator, whose input is the angular speed ω and output torque τ, is said to be passive if it satisfies that:

$$E(t) - E(0) = \int_0^t \omega(\sigma)\tau(\sigma)d\sigma \geq 0 \quad \forall t \geq 0 \tag{7}$$

where $E(t)$ is the energy of the servo, $E(0)$ is the initial energy, and the product $\omega \cdot \tau$ is the instantaneous power. As stated in [23], the passivity can be defined at both sides of the compliant transmission, so we can exploit the feedback provided by the FDA servos with no need for additional sensors at the load side. The energy of the FDA at the leader side, expressed in discrete time, is thus computed as follows:

$$E_{FSA}(n) = E_{FSA}(n-1) + T\,\omega_{FSA}(n-k_b)\tau_{FSA}(n-k_b) \tag{8}$$

where T is the sampling period. The instantaneous power, corresponding to the second term in the right side of Eq. (8), will be analyzed at the LDA to evaluate the passivity of the system during the interaction phases of the operation, as it will be seen in Section V-C.

V. EXPERIMENTAL RESULTS

A. Benchmarking with Industrial Task Board

The goal of this first experiment is to benchmark the developed teleoperation system in the realization of a manipulation task requiring a certain level of accuracy, coordination, and dexterity, using for this purpose the industrial task board presented in [26] (ref. [37] collects several benchmark results with it). The experimental setup and the conducted operation are illustrated in Figure 5 and can be followed in the video attachment. The FDA is placed in front of the task board while the human operator is handling the LDA next to it. The operation consists of seven tasks, indicated in Table I along with the execution time. Tasks 1, 2, and 6 presented a low difficulty, whereas Task 4 required the use of both arms to lift and push the door case, a tricky operation. The realization of Tasks 2, 3 and 5 depends mainly on accurate end effector positioning. The evolution of the left/right arms tool center point (TCP) position is represented in Figure 6.

TABLE I

EXECUTION TIME OF THE TASK BOARD BENCHMARK

#	Task	FDA arm(s)	Time [s]	Accuracy [mm]
1	Press Start button	Left	4.5	10
2	Move slider up	Left	8.8	5
3	Move slider down	Left	3.5	5
4	Open case door	Left + Right	14.5	
5	Insert probe	Right	11.9	3
6	Close case door	Right	2	-
7	Press Stop button	Right	3.8	10

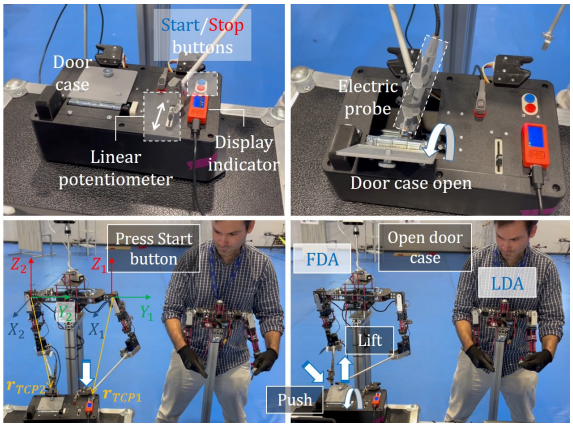

Fig. 5. Industrial task board used for benchmarking the LiCAS teleoperation system (up). Realization of the test with the LDA.

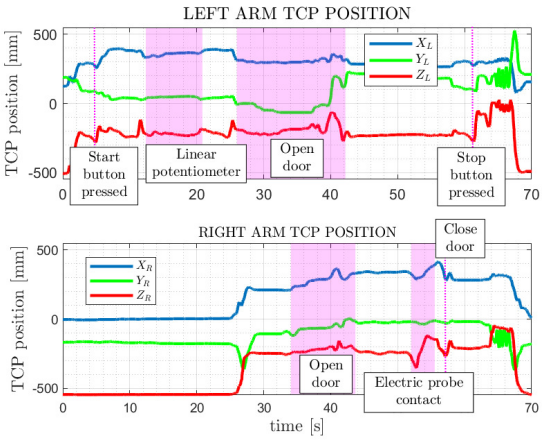

Fig. 6. Tool center point (TCP) position of left and right arms during the execution of the task board benchmark, indicating the seven phases.

B. Replication of Dexterous Manipulation Skills

The goal of this experiment is to validate the developed teleoperation system through the realization of a complex bimanual manipulation task consisting in the installation of an helical bird flight diverter on a power line section. The complexity of the operation, represented in Figure 7, is due to the geometry and elasticity of this device, extensively used on the Spanish power grid to avoid the collision of birds (see [28]). The cable suspended configuration of the arms, depicted in Figure 8, simulates the operation from a crane to reach the power line. The execution of the task can be seen in the video attachment, representing in Figure 9 the trajectory of both arms along with the evolution of the joints position and PWM. The gripper state indicates the instant when the left arm grabs/releases the device to wrap it around the cable.

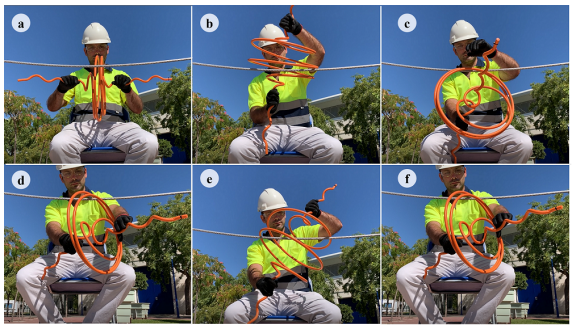

Fig. 7. Human operator installing an helical bird diverter on a power line.

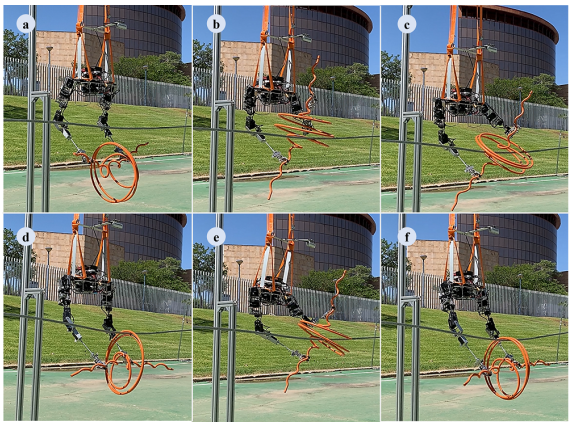

Fig. 8. Dual arm robot conducting the device installation by teleoperation.

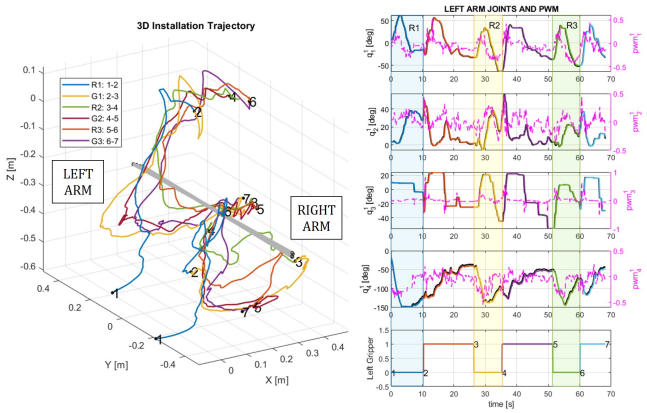

Fig. 9. 3D trajectory followed by the FDA in the installation of the helical bird diverter (left). Evolution of joint position, PWM, and gripper state of the left arm, indicating the three rolling maneuvers of the device (right).

C. Bilateral Teleoperation Validation

This experiment aims to validate the bilateral teleoperation scheme presented in Section 4-C, proving its capacity to transfer haptic feedback to the human operator. The task

TABLE II

PHASES INVOLVED IN THE INSTALLATION OF THE HELICAL DEVICE.

Phase	Steps	Duration [s]	Description
R_1	a, b, c	10	Insertion of the helical diverter.
G_1	d	17	First grasping of the left branch.
R_2	e	8	First rolling around the power line.
G_2	f	17	Second grasping of the left branch.
R_3	e	8	Second wrap around power line.
G_3	f	8	Third grasping of the left branch.

consist of grasping the power line used in previous test with the left arm, and force a pushing/pulling effort against it. In order to avoid the overload of the FDA servos, the operator will employ the kinesthetic feedback to accommodate the force exerted by the arm, which involves mainly the shoulder and elbow flexion/extension joints. Figure 10 represent the position, speed, PWM, and power of the joints for joints q_{11}^L and q_{14}^L, respectively. The instant power of the servos is computed and represented, identifying with yellow shaded areas the time instants when the passivity is not satisfied due to the interaction forces. In the first interaction, the cable is pulled backwards, involving mainly q_{11}^F, and then, after returning to a nominal position, the cable is pulled downwards, involving mainly q_{14}^F. The graphs show how the power becomes negative when the torque (PWM) is opposed to the angular speed, a situation that is translated by the LSA controler into opposing the HOP movements, providing the haptic feedback that indicates the user the arm overload.

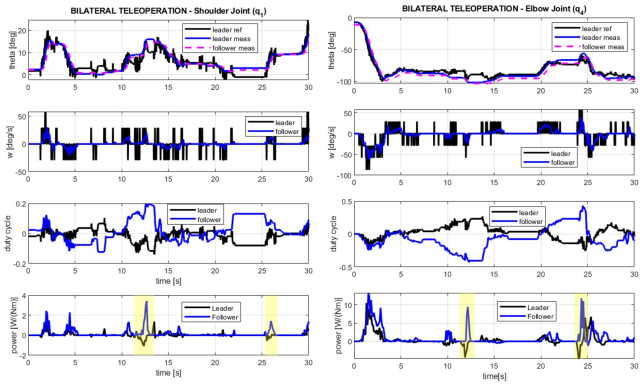

Fig. 10. Position, speed, PWM and power of the shoulder and elbow flexion/extension joints in the bilateral teleoperation test. Yellow areas indicate instants in which the user feels the pushing/pulling force exerted by the left arm against the obstacle.

D. Validation in Aerial Manipulation Tasks

Finally, the teleoperation system has been validated in two flight tests. On the one hand, the instalation of the helical bird diverter has been partially replicated on flight, as shown in Figure 1, integrating the FDA in a medium scale multi-rotor flying in the GRVC Indoor Testbed, equipped with an Opti-Track positioning system. On the other hand, a parcel load and drop operation has been conducted in a logistics scenario, represented in Figure 11. The execution of both experiments can be seen in the video attachment.

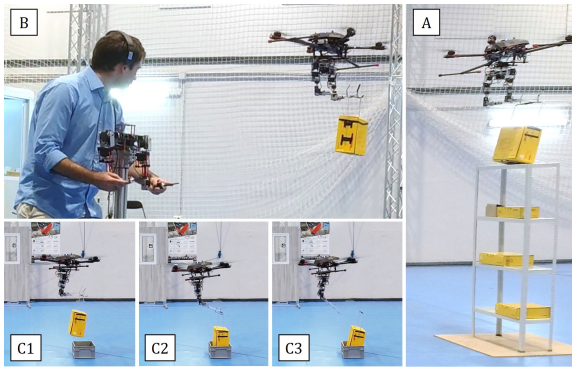

Fig. 11. Evaluation of the dual arm teleoperation system in an aerial manipulation logistics operation involving the grasping and drop of a parcel.

VI. CONCLUSIONS AND FUTURE WORK

This paper presented a bilateral teleoperation system for the realization of complex bimanual manipulation tasks that allows to replicate the human skills by using an anthropomorphic leader-follower configuration. The very low weight of the arms (1.0 / 2.5 kg) facilitates the deployment of the system on site, whereas the human-size and human-like kinematics allow their integration in multi-rotor platforms for the realization of aerial manipulation tasks, as well as their use in ground service applications, evaluated through a benchmarking task board. The mechanical compliance of the follower provides passive accommodation of the robot to the interaction forces raised during the installation process, exploiting the measurements given by the smart servos to provide kinesthetic feedback to the operator. The presented experiments serve to illustrate how this interface could be used for teaching the robot to conduct complex manipulation tasks by demonstration.

As future work, it is considered extending the kinematics of the leader dual arm by incorporating a joystick interface at the forearm so the human operator can control the rotation of the wrist joints, as well as a torso mechanism to allow upper-body teleoperation of humanoid robots. Making the LDA wearable, along with the use of a headset for displaying the point of view of the follower dual arm, makes this system interesting for a number of field robotic applications requiring the transfer of cognitive skills of human workers to the robotic arms, while the haptic feedback may be useful for assisting the operation and increase the situational awareness of the operator.

ACKNOWLEDGMENT

This work has been funded by the European Commission through the European ROBotics and AI Network (euROBIN, Grant agreement ID: 101070596), by the AERIAL COgnitive integrated multi-task Robotic system with Extended operation range and safety (AERIAL-CORE, Grant agreement ID: 871479) project, and by the AEROTRAIN Marie Skłodowska-Curie project (MSCA-ITN-2020-953454).

REFERENCES

[1] T. B. Sheridan, "Space teleoperation through time delay: Review and prognosis," *IEEE Transactions on robotics and Automation*, vol. 9, no. 5, pp. 592–606, 1993.

[2] W.-K. Yoon, T. Goshozono, H. Kawabe, M. Kinami, Y. Tsumaki, M. Uchiyama, M. Oda, and T. Doi, "Model-based space robot teleoperation of ets-vii manipulator," *IEEE Transactions on Robotics and Automation*, vol. 20, no. 3, pp. 602–612, 2004.

[3] J. Artigas, R. Balachandran, M. De Stefano, M. Panzirsch, R. Lampariello, A. Albu-Schaeffer, J. Harder, and J. Letschnik, "Teleoperation for on-orbit servicing missions through the astra geostationary satellite," in *2016 IEEE Aerospace Conference*, pp. 1–12, IEEE, 2016.

[4] J. Lee, R. Balachandran, Y. S. Sarkisov, M. De Stefano, A. Coelho, K. Shinde, M. J. Kim, R. Triebel, and K. Kondak, "Visual-inertial telepresence for aerial manipulation," in *2020 IEEE International Conference on Robotics and Automation (ICRA)*, pp. 1222–1229, IEEE, 2020.

[5] J. Lee, R. Radhakrishna Balachandran, K. Kondak, A. Coelho, M. De Stefano, M. Humt, J. Feng, T. Asfour, and R. Triebel, "Virtual reality via object pose estimation and active learning: Realizing telepresence robots with aerial manipulation capabilities," *Field Robotics*, vol. 3, pp. 323–367, 2023.

[6] K. Darvish, L. Penco, J. Ramos, R. Cisneros, J. Pratt, E. Yoshida, S. Ivaldi, and D. Pucci, "Teleoperation of humanoid robots: A survey," *IEEE Transactions on Robotics*, 2023.

[7] W. Si, N. Wang, and C. Yang, "A review on manipulation skill acquisition through teleoperation-based learning from demonstration," *Cognitive Computation and Systems*, vol. 3, no. 1, pp. 1–16, 2021.

[8] A. Suarez, G. Heredia, and A. Ollero, "Design of an anthropomorphic, compliant, and lightweight dual arm for aerial manipulation," *IEEE Access*, vol. 6, pp. 29173–29189, 2018.

[9] A. Suarez, A. E. Jimenez-Cano, V. M. Vega, G. Heredia, A. Rodriguez-Castaño, and A. Ollero, "Design of a lightweight dual arm system for aerial manipulation," *Mechatronics*, vol. 50, pp. 30–44, 2018.

[10] A. Suarez, S. R. Nekoo, and A. Ollero, "Ultra-lightweight anthropomorphic dual-arm rolling robot for dexterous manipulation tasks on linear infrastructures: A self-stabilizing system," *Mechatronics*, vol. 94, p. 103021, 2023.

[11] D. Q. Truong, B. N. M. Truong, N. T. Trung, S. A. Nahian, and K. K. Ahn, "Force reflecting joystick control for applications to bilateral teleoperation in construction machinery," *International Journal of Precision Engineering and Manufacturing*, vol. 18, pp. 301–315, 2017.

[12] A. Coelho, Y. Sarkisov, X. Wu, H. Mishra, H. Singh, A. Dietrich, A. Franchi, K. Kondak, and C. Ott, "Whole-body teleoperation and shared control of redundant robots with applications to aerial manipulation," *Journal of Intelligent & Robotic Systems*, vol. 102, pp. 1–22, 2021.

[13] V. Girbes-Juan, V. Schettino, Y. Demiris, and J. Tornero, "Haptic and visual feedback assistance for dual-arm robot teleoperation in surface conditioning tasks," *IEEE Transactions on Haptics*, vol. 14, no. 1, pp. 44–56, 2020.

[14] A. Talasaz, A. L. Trejos, and R. V. Patel, "The role of direct and visual force feedback in suturing using a 7-dof dual-arm teleoperated system," *IEEE transactions on haptics*, vol. 10, no. 2, pp. 276–287, 2016.

[15] J. Bimbo, C. Pacchierotti, M. Aggravi, N. Tsagarakis, and D. Prattichizzo, "Teleoperation in cluttered environments using wearable haptic feedback," in *2017 IEEE/RSJ International Conference on Intelligent Robots and Systems (IROS)*, pp. 3401–3408, IEEE, 2017.

[16] D. Prattichizzo, F. Chinello, C. Pacchierotti, and M. Malvezzi, "Towards wearability in fingertip haptics: a 3-dof wearable device for cutaneous force feedback," *IEEE Transactions on Haptics*, vol. 6, no. 4, pp. 506–516, 2013.

[17] Y. Ishiguro, T. Makabe, Y. Nagamatsu, Y. Kojio, K. Kojima, F. Sugai, Y. Kakiuchi, K. Okada, and M. Inaba, "Bilateral humanoid teleoperation system using whole-body exoskeleton cockpit tablis," *IEEE Robotics and Automation Letters*, vol. 5, no. 4, pp. 6419–6426, 2020.

[18] M. Mallwitz, N. Will, J. Teiwes, and E. A. Kirchner, "The capio active upper body exoskeleton and its application for teleoperation," in *Proceedings of the 13th Symposium on Advanced Space Technologies in Robotics and Automation. ESA/Estec Symposium on Advanced Space Technologies in Robotics and Automation (ASTRA-2015). ESA*, 2015.

[19] M. H. M. Zaman, M. F. Ibrahim, N. Zainal, and M. F. Nasir, "Dual-arm robot with mobile robot platform with master-slave configuration for teleoperation application," *Int J*, vol. 9, pp. 1–4, 2020.

[20] F. Zorić, A. Suarez, G. Vasiljević, M. Orsag, Z. Kovačić, and A. Ollero, "Performance comparison of teleoperation interfaces for ultra-lightweight anthropomorphic arms," in *2023 IEEE/RSJ International Conference on Intelligent Robots and Systems (IROS)*, pp. 7026–7033, IEEE, 2023.

[21] M. Capurso, M. M. G. Ardakani, R. Johansson, A. Robertsson, and P. Rocco, "Sensorless kinesthetic teaching of robotic manipulators assisted by observer-based force control," in *2017 IEEE International Conference on Robotics and Automation (ICRA)*, pp. 945–950, IEEE, 2017.

[22] M. Ragaglia, A. M. Zanchettin, L. Bascetta, and P. Rocco, "Accurate sensorless lead-through programming for lightweight robots in structured environments," *Robotics and Computer-Integrated Manufacturing*, vol. 39, pp. 9–21, 2016.

[23] H. Lee, J.-H. Ryu, J. Lee, and S. Oh, "Passivity controller based on load-side damping assignment for high stiffness controlled series elastic actuators," *IEEE Transactions on Industrial Electronics*, vol. 68, no. 1, pp. 871–881, 2020.

[24] A. Suarez, F. Real, V. M. Vega, G. Heredia, A. Rodriguez-Castaño, and A. Ollero, "Compliant bimanual aerial manipulation: Standard and long reach configurations," *IEEE Access*, vol. 8, pp. 88844–88865, 2020.

[25] I. Armengol, A. Suarez, G. Heredia, and A. Ollero, "Design, integration and testing of compliant gripper for the installation of helical bird diverters on power lines," in *2021 Aerial Robotic Systems Physically Interacting with the Environment (AIRPHARO)*, pp. 1–8, IEEE, 2021.

[26] P. So, J. Wittmann, P. Ruhkamp, A. Sarabakha, and S. Haddadin, "Towards remote robotic competitions: An internet-connected task board and dashboard," *arXiv preprint arXiv:2201.09565*, 2022.

[27] A. Ollero, M. Tognon, A. Suarez, D. Lee, and A. Franchi, "Past, present, and future of aerial robotic manipulators," *IEEE Transactions on Robotics*, vol. 38, no. 1, pp. 626–645, 2021.

[28] J. Cacace, S. M. Orozco-Soto, A. Suarez, A. Caballero, M. Orsag, S. Bogdan, G. Vasiljevic, E. Ebeid, J. A. A. Rodriguez, and A. Ollero, "Safe local aerial manipulation for the installation of devices on power lines: Aerial-core first year results and designs," *Applied Sciences*, vol. 11, no. 13, p. 6220, 2021.

[29] D. Pinzon, R. Vega, Y. P. Sanchez, and B. Zheng, "Skill learning from kinesthetic feedback," *The American Journal of Surgery*, vol. 214, no. 4, pp. 721–725, 2017.

[30] A. Suárez, P. Sanchez-Cuevas, M. Fernandez, M. Perez, G. Heredia, and A. Ollero, "Lightweight and compliant long reach aerial manipulator for inspection operations," in *2018 IEEE/RSJ International Conference on Intelligent Robots and Systems (IROS)*, pp. 6746–6752, IEEE, 2018.

[31] X. Hou, R. Mahony, and F. Schill, "Comparative study of haptic interfaces for bilateral teleoperation of vtol aerial robots," *IEEE Transactions on Systems, Man, and Cybernetics: Systems*, vol. 46, no. 10, pp. 1352–1363, 2015.

[32] M. Mohammadi, A. Franchi, D. Barcelli, and D. Prattichizzo, "Cooperative aerial tele-manipulation with haptic feedback," in *2016 IEEE/RSJ International Conference on Intelligent Robots and Systems (IROS)*, pp. 5092–5098, IEEE, 2016.

[33] G. A. Yashin, D. Trinitatova, R. T. Agishev, R. Ibrahimov, and D. Tsetserukou, "Aerovr: Virtual reality-based teleoperation with tactile feedback for aerial manipulation," in *2019 19th International Conference on Advanced Robotics (ICAR)*, pp. 767–772, IEEE, 2019.

[34] V. Lippiello, J. Cacace, A. Santamaria-Navarro, J. Andrade-Cetto, M. A. Trujillo, Y. R. R. Esteves, and A. Viguria, "Hybrid visual servoing with hierarchical task composition for aerial manipulation," *IEEE Robotics and Automation Letters*, vol. 1, no. 1, pp. 259–266, 2015.

[35] N. Imanberdiyev, S. Sood, D. Kircali, and E. Kayacan, "Design, development and experimental validation of a lightweight dual-arm aerial manipulator with a cog balancing mechanism," *Mechatronics*, vol. 82, p. 102719, 2022.

[36] A. Albu-Schäffer, C. Ott, and G. Hirzinger, "A unified passivity-based control framework for position, torque and impedance control of flexible joint robots," *The international journal of robotics research*, vol. 26, no. 1, pp. 23–39, 2007.

[37] "euRobin WP1 Collection." `https://github.com/peterso/euROBIN_WP1_collection`. [Online; Accessed: 2024-02-24].